Available online at www.sciencedirect.com
SCIENCE DIRECT
Journal of Hydrology xx (xxxx) 1–19
Journal of Hydrology
www.elsevier.com/locate/jhydrol

Dynamics of floodplain-island groundwater flow in the Okavango Delta, Botswana

P. Wolski[a,*], H.H.G. Savenije[b,c]

[a]*Harry Oppenheimer Okavango Research Centre, University of Botswana, P/Bag 285, Maun, Botswana*
[b]*UNESCO-IHE, Institute for Water Education, P.O. Box 3015, 2601 DA, Delft, The Netherlands*
[c]*Delft University of Technology, P.O. Box 5048, 2600 GA Delft, The Netherlands*

Received 10 May 2005; revised 23 May 2005

Abstract

Surface water-groundwater interactions play a crucial role in the hydrology and ecology of the Okavango Delta. The hydrology of the Delta is dominated by the annual arrival of a flood wave which is distributed over an number of branches. Subsequently, the flood water feeds the phreatic aquifers underlying the Delta islands. In order to evaluate the seasonal and long-term dynamics of the surface water-groundwater interactions between the floodplains and the islands, a network of piezometers located in various locations of the Delta was monitored. Groundwater table fluctuations observed for up to 6 years were analysed and modelled using groundwater flow models. The floodplain-island groundwater flow is in general very dynamic and driven by island evaporation and transpiration. A typical small to medium sized island (width <500 m), appear not to be influenced by long-term antecedent conditions. Only on large islands (width >500 m) and at the perimeter of the flooded area is the influence of long-term antecedent conditions apparent. The knowledge gained during this study will be used for the improvement of the hydrological and hydro-ecological model of the Delta, and can be useful for the description of floodplain dynamics in semi-arid regions in general.

Keywords: Surface water-groundwater interaction; Floodplain dynamics; Wetlands hydrology; Okavango Delta; Groundwater modelling; Water balance

1. Introduction

Surface water–groundwater (SW–GW) interactions, or infiltration and exfiltration processes, are important processes in the hydrology and ecology of wetlands. Wetlands are generally linked to groundwater (Mitsch and Gosselink, 2000); one can distinguish wetlands dominated by groundwater discharge, by groundwater recharge or flow-through wetlands. The nature of interactions between surface water and groundwater, i.e. direction and magnitude of the water flux, is a result of a complex interplay of climate, morphology, soils, geology, vegetation and hydrology of a system (Sophocleous, 2002; Winter, 1999; Woessner, 2000). Work of Meyboom (1967) and Winter (1999) shows that subtle changes in

* Corresponding author. Tel./fax: +267 686 1833.
E-mail addresses: pwolski@mopipi.ub.bw (P. Wolski), hsa@ihe.nl (H.H.G. Savenije).

0022-1694/$ - see front matter © 2005 Elsevier B.V. All rights reserved.
doi:10.1016/j.jhydrol.2005.07.027

groundwater table driven by recharge, evaporation from groundwater and surface water level fluctuations can cause considerable seasonal variation in magnitude and direction of SW–GW fluxes. The direction and magnitude and direction of the SW–GW flux is important for bio-chemistry of the wetland (LaBaugh et al., 1987) and particularly for biological and biochemical processes occurring at the water-soil interface, or hyporheic zone (Brunke and Gonser, 1997). SW–GW interactions are also one of the pathways of exposure of wetlands to pollution and degradation by groundwater exploitation (Suso and Llamas, 1993).

The dynamics of the interactions between surface water and groundwater often determine the wetland's hydroperiod or the duration, extent and depth of inundation (Mitsch and Gosselink, 2000). A striking example is that of prairie pothole wetlands in US and Canada, where SW–GW interaction, as determined by geology and topography, is one of the main factors causing differences in duration of inundation between various potholes ranging from episodic to permanent (Winter and Rosenberry, 1995). In seasonally inundated alluvial plain wetlands, SW–GW interaction causes modification of the wetland's hydroperiod through recharge of shallow groundwater during flood propagation, and, after flood recession, release of water from bank storage (e.g. Weng et al., 2003).

SW–GW interaction causes the groundwater in the vicinity of a wetland to be functionally related to the wetland itself, leading to an ecological framework where the riparian vegetation is considered part of the wetland (Tiner, 1999). In this setting, the dynamics of SW–GW fluxes can affect the ecology of the riparian vegetation (Hughes, 1990), and on the other hand, the riparian vegetation can influence wetland's hydrology through transpirative uptake of groundwater (Doss, 1993; Sacks et al., 1992; Winter and Rosenberry, 1995).

In this paper we focus on the seasonal dynamics of hydrological interactions between seasonal floodplains and islands in the Okavango Delta. We do it on the basis of observations of groundwater table fluctuations and modelling of floodplain-island groundwater flow at two sites, representing typical Okavango Delta islands. Additionally, by simulating hypothetical conditions of prolonged flooding and no-flood situations, we assess the inter-annual dynamics of surface water-groundwater flows at these sites. By this work we contribute to the quantitative understanding of 'losses' of floodwater and of factors affecting the spatial and temporal variability of the hydrological system in the Okavango Delta. In this way we make the contribution to the improvement of the hydrological model of the Delta, which in the past did not account for the lateral groundwater fluxes and their role on the system's water balance. Also, we assess the impact of floodplain dynamics on the riparian vegetation. In a broader sense, we provide a quantitative description of surface water-groundwater interactions in a floodplain system dominated by groundwater recharge, examples of which are few in the literature.

2. The Okavango Delta

The Okavango Delta (Fig. 1) is a large inland wetland created by the Okavango river. Morphologically, the Okavango Delta is a mosaic of flat broad floodplains and round to shapeless islands ranging in size from several square meters to 500 km^2. The principal hydrological feature of the Okavango Delta is the seasonal flood stemming from the Okavango river catchment in Angola, and to a lesser extent local rainfall. The area covered by water expands from its annual low of 2500–4000 km^2 in February–March to its annual high of 6000–12000 km^2 in August–September (McCarthy et al., 2004). The seasonality of inundation is the basis for distinguishing three major hydro-ecological zones, namely: permanent swamp, seasonal (regularly flooded) floodplains and occasional floodplains. The flood cycle is out of phase with the rainy season, which occurs between November and March.

The Okavango river drains a basin underlain by highly weathered Kalahari sands (Thomas and Shaw, 1991), and thus the majority of the sediment carried into the Delta is composed of fine to medium sand with a small proportion ($<5\%$) of the finer fractions (McCarthy and Ellery, 1995). As a consequence, floodplains in the Okavango

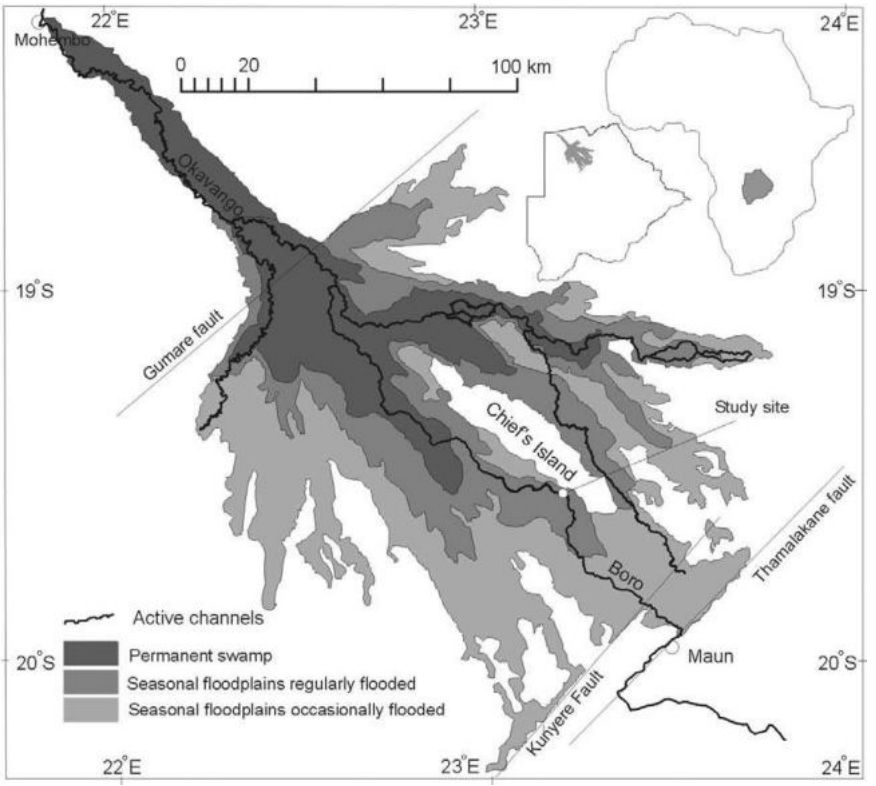

Fig. 1. Location and main features of the Okavango Delta, Botswana.

Delta are predominantly sandy, although surface layers may contain fine alluviums and chemical precipitates from groundwater. Accumulation of organic material is insignificant in the seasonally flooded zone due to dry season fires and removal of ash by wind (Krah et al., 2004; Hogberg et al., 2002). Islands in the Okavango Delta are usually built of fine, clayey-like material, forming lenses roughly 3–15 m thick, and usually underlain by clean parent sands. The material is composed of amorphous silica and carbonates which precipitate from island groundwater as a result of evaporative enrichment (McCarthy et al., 1991; McCarthy, 2005).

The Okavango Delta is covered with vegetation that reflects local hydrological conditions (Ellery and Ellery, 1997). Permanently flooded areas support obligate aquatic plants such as papyrus (*Cyperus papyrus*). Seasonally flooded areas support emergent aquatic sedges, while drier, occasionally inundated plains, support grasses. Island and dry-land vegetation can broadly be divided into semi-deciduous riparian forest and dry-land forest. Riparian forest composed of phreatophytic species occupies fringes of islands, where flooding does not occur, but groundwater is fresh and shallow. Due to groundwater salinization, the central area of such islands supports only salinity resistant grasses. Dry-land forest is rain-fed and occupies larger land bodies, where groundwater is deep.

The climate of the region of the Okavango Delta is semi-arid with 460 mm a^{-1} of rainfall and one distinct rainy season from November to March. Class A pan evaporation (with appropriate, seasonally-varying pan coefficient) amounts to 1800 mm a^{-1}. Maximum monthly rates of 250 mm $month^{-1}$ occur in October and minimum of 90–100 mm $month^{-1}$ occur in June/July. There is a slight regional gradient of rainfall and potential evaporation. Both decrease towards the southwest.

3. Study sites

3.1. Camp Island

Camp Island is a relatively large (approximately 400 by 1500 m) and elongated island, located in the regularly flooded zone adjacent to the main channel of Boro river (Fig. 2). Annual surface water level fluctuations vary between 0.8 and 1.5 m. Camp Island has a relatively wide (100 m) vegetated fringe composed of riparian woodland. The island's centre is covered by grassland. The island is underlain by a relatively thick (more that 7 m) lens of deposits of predominantly clayey texture.

3.2. Phelo's floodplain and Pan floodplain

Phelo's floodplain site comprises a narrow floodplain and the bordering islands (Fig. 2). The one located to the NE of the floodplain is Chief's Island, the largest in the Delta. Its central part is covered by a typical dry-land forest, while adjacent to the floodplains, a mixture of dry-land and riparian species occurs. The substratum penetrated by piezometers W1–W8 and P1–P4 (up to 8 meters) is uniformly sandy, apart from a small clayey lens in the central part of the floodplain. Phelo's floodplain is annually flooded, however, but the duration and level of the floods vary between years. Annual surface water level fluctuations vary between 0.8 and 1.5 m.

To the east of Phelo's floodplain there is another floodplain system containing a relatively deep pan (hence called Pan floodplain), which is separated from Phelo's floodplain by a topographic threshold. The Pan floodplain is only flooded if the water level of Phelo's floodplain exceeds that threshold. Between 1997 (beginning of observations) and 2003 this happened only in 2000 and 2001. The floodplain is mostly sandy (piezometers F, G and Pn1, Pn2), but the pan is underlain by clayey deposits. Piezometer Pn3 drilled in the main body of Chief's island penetrated clean and slightly calcretized sands.

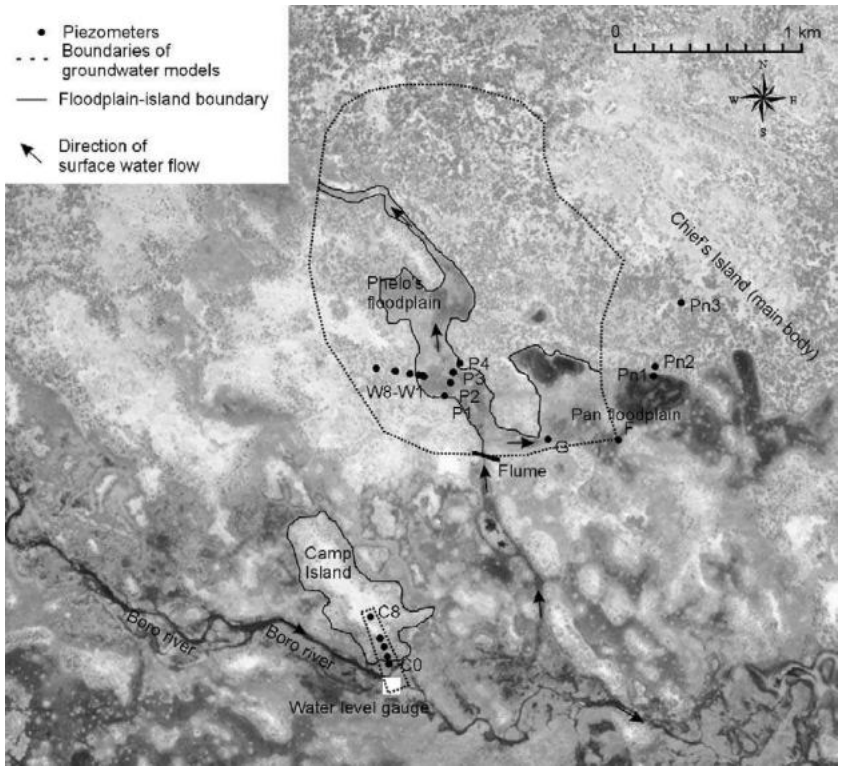

Fig. 2. Location of Observation Island, Camp Island, Phelo's and Pan floodplains. Background: aerial photo.

4. Materials and methods

4.1. Piezometric network

Groundwater table fluctuations were observed through a network of piezometers made of 25.4 mm PVC pipes installed in hand-augered holes, 2–11 m deep. The bottom part of the pipes was slotted and covered with several layers of filter material (vylene non-woven and agritex) over a length of 1 m. The pipes were cut at ground level to prevent destruction by elephants and baboons and covered with a cap. The cap was not hermetically closed to prevent build up of pressure inside the piezometer during phases of fast groundwater rise. The disadvantage of this solution is that the piezometers drilled within the inundated area were submerged at the arrival of the flood. The piezometers were linked to reference benchmarks through combined GPS (TRIMBLE 4700) and theodolite (LEICA 2300) surveying. The method provided accuracy of absolute height determination within 0.5 cm with respect to the benchmarks.

Groundwater levels were monitored on a biweekly basis, although at some locations measurements were less regular due to accessibility problems. Observation periods varied between 1 and 5 years. Measurements were done from the top of the piezometer pipe using a manual sounding device with the accuracy of about 0.5 cm. In several piezometers automatic groundwater loggers (DIVER) were installed which recorded the groundwater level every 30 min.

Aquifer conductivity was tested in all piezometers using a slug test method. Piezometers were topped with water and recession of groundwater table was measured using a water level logger. In each of the piezometers three consecutive tests were made. The results were interpreted using the Hvorslev method (Kruseman, 1981) and the values of the three tests were averaged (Table 1).

4.2. Soil hydraulic parameters

To obtain information on the range of hydraulic parameters of island deposits, undisturbed soil samples were taken from several locations on Camp Island. They were taken from the bottom of hand-augered holes by pushing in PVC cylinders of 5 cm diameter and 10 cm height. Cylinders were sealed and transported to the laboratory. Hydraulic conductivity was measured using the standard falling head permeameter method (Freeze and Cherry, 1979). After the test, the saturated samples were weighted and subsequently oven-dried to 105 °C for 24 h and weighed again. Total porosity of the samples was obtained from the difference in weight and volume of the cylinder.

4.3. Water balance of the Phelo's floodplain

The water balance of Phelo's floodplain was calculated earlier by Ramberg et al. (2005). For obtaining the water balance, surface water inflow was measured at the flume site (Fig. 2). Evaporation was calculated based on the extent of the flooded area using Penman's formula for open water evaporation (Maidment, 1992). The water level-volume relationship obtained from the topographic map was used to

Table 1
Summary of hydraulic properties tested in the studied sites

Type	Site	Lithology	Hydraulic conductivity average[a] (range) (m d^{-1})	Total porosity average (range) (–)	Number of samples
Slug tests	Phelo's site W1–W8	Sandy	8.4 (4.2–11.5)		3
	Camp Island	Clay lens	0.34 (0.11–0.67)		6
Pump test	Phelo's floodplain[b]	Sandy	19.68 (13.4–27.1)		5
Permeameter	Phelo's floodplain[b]	Sandy	4.05 (0.02–35.41)	33 (25–38)	19
	Camp Island	Clay lens	0.0014 (<0.00001–0.11)	37 (21–59)	50

[a] Geometric mean.
[b] Results taken from Obakeng and Gieske (1997).

calculate the change in floodplain storage. Infiltration to groundwater was calculated as a residual term of the water balance equation.

Original data of Ramberg et al. (2005) cover the seasons of 1997–1999, when only Phelo's floodplain was inundated. It was attempted to extend the water balance calculations to the 2000–2001 seasons when the Pan floodplain was inundated as well. However, there is a limited knowledge of distribution of flood in the Pan floodplain. The Pan floodplain fills-up slowly, and the relationship between the water level at the floodplain inlet and the flood area and floodplain volume could not be established. As a consequence, evaporation and floodplain storage could not be determined with sufficient accuracy and the total inflow to Phelo's and Pan floodplain systems during those two years could not be separated into water balance components. Calculations were, however, performed for 2002 (Table 2), when only the Phelo's floodplain was flooded. The results are used in calibration of Phelo's floodplain groundwater model.

4.4. Groundwater flow modelling

Groundwater flow models were run for the Camp Island and for the Phelo's floodplain using the MODFLOW code (McDonald and Harbaugh, 1988) with PMWIN 5.0 (Chiang and Kinzelbach, 2001) pre- and postprocessor. The models are transient, and were calibrated manually against observed time series of groundwater levels and floodplain flow discharges. The models represent the principal processes that influence groundwater flows in the floodplain-island system: variation of the flood level and lateral expansion of the flood, as well as evaporation and transpiration from groundwater.

The variation of the flood level and the lateral expansion of the flood was simulated using a head-dependent flow boundary condition represented in MODLFOW by the river package. A simulation period was divided into so-called stress periods reflecting the variation in surface water levels. For each of the stress periods, the extent of the flood was obtained from the topographic cross-section and the measured surface water levels. The number of river package cells in each of the stress periods corresponds to the extent of the flooding during that period.

Evaporation and transpiration from groundwater were modelled using the evaporation package of MODFLOW. This package relates the evaporation flux from the groundwater table to the depth of the groundwater table. Evaporation varies linearly between the maximum flux depth (taken at ground surface level) and zero flux depth, or so-called extraction depth.

In the models, only local groundwater flow systems were taken into consideration, i.e. a system comprising a floodplain and an adjacent island, disregarding larger scale regional flows. This was done in spite of the fact that the Okavango Delta forms a regional groundwater mound, which seems to suggest the presence of regional groundwater flow (see for example McCarthy, 2005). However, in an earlier regional modelling exercise by Wolski and Savenije (2003) it was established that with

Table 2
Water balance for the Phelo's floodplain, after Ramberg et al. (2005), extended to cover 2002 flood season

			1997	1998	1999	2002
Inflow		(m^3/season)	1388000	494000	1422000	1076000
Evaporation		(m^3/season)	164500	45800	142600	184000
Infiltration	Total	(m^3/season)	1223300	448300	1279000	866000
	Total[a]	(mm a^{-1})	7430	4680	9750	4300
	Average	(mm d^{-1})	46	52	54	29
	Maximum	(mm/10 days)	1140	1110	1740	570
Infiltration/ inflow ratio		(–)	0.88	0.91	0.90	0.81
Infiltration/evaporation ratio		(–)	7.4	9.8	9.0	4.7

[a] Calculated over the time-varying area of open water surface.

aquifer thickness and properties assumed to favour regional flows (300 m deep layer of uniform sands characterized by hydraulic conductivity of 20 m d^{-1}), the drainage by a regional groundwater flow systems did not exceed 1 mm a^{-1}. As a result it was concluded that groundwater flows are dominated by local flow systems. This is not surprising in view of the extremely low regional gradient (~1:4000) as opposed to relatively large local gradients (1:100 to 1:200).

4.5. Assessment of short term and long term dynamics of floodplain-island groundwater fluxes

The calibrated models were used to study the short-term (seasonal) variation of floodplain-island groundwater flow. In order to assess to what extent the flow is influenced by antecedent conditions extending beyond one year, two hypothetical situations were simulated by the models. The first situation represents a lack of flood for a prolonged period of time and the subsequent return to a 'normal' flooding pattern; the second situation represents a prolonged period of high floods with a subsequent return to a 'normal' flooding pattern.

The time series used in the calibration runs was used to represent the 'normal' flooding pattern. To simulate a no-flood condition, a period with no floods was introduced as the antecedent condition for that 'normal' flood sequence. To create the desired antecedent conditions, no water was supplied to the modelled domain during a prolonged period, i.e. no river package cells were implemented for a relevant amount of time steps. Under such conditions, evaporation and transpiration were driving the groundwater table decline in the model. Four simulations were made with a no-flood period at 1, 2, 3 and 10 years respectively.

To simulate a prolonged high flood condition a steady-state model was used with the same parametrization as in the calibrated version of the transient model, with the floodplain water level set at the highest flood on record. The obtained groundwater table is assumed to be the maximum possible storage of the island aquifer. This groundwater table was subsequently used as the initial groundwater table in a transient simulation of the 'normal' flood sequence.

5. Results and analyses of field measurements

5.1. Hydraulic properties of the groundwater aquifers

There is a considerable difference in hydraulic conductivity between the island lens material and the sands beneath the lens and in the floodplains (Table 1). The sands are characterized by high total porosity (in order of 25–38%), and contain very little clay. Not surprisingly, they display high hydraulic conductivities-up to 35 m d^{-1}. Lens material samples taken from the top 3 m of Camp Island are characterized by a total porosity in the order of 21–59%, but due to the high content of clay fraction have low hydraulic conductivity. Values of 0.11–0.67 m d^{-1} were obtained from slug tests, and values of 0.00001–0.11 m d^{-1} were obtained in laboratory tests. The large difference between the methods may be the result of laboratory method measuring only vertical conductivity, while slug tests measure horizontal conductivity. In addition, samples for laboratory tests were taken from the zone above the groundwater table, which demonstrate a larger degree of cementation by precipitates, and thus demonstrate lower conductivity than the zone sampled by slug tests. In the woodlands surrounding the Phelo's floodplain, higher conductivity values, comparable with those of the floodplain sediments, were obtained.

5.2. Groundwater table fluctuations

5.2.1. Camp Island

Under Camp Island, groundwater is 1–3 m below ground level in the riparian zone, and 2.5–4 m in the island's central grassland (Fig. 3). The annual flood is the main event driving fluctuations of the groundwater table. The groundwater table within the riparian zone reacts very fast to the arrival of the flood. A rise in piezometers 150–200 m away from the floodplain is observed within several days after the arrival of the flood. The groundwater table stabilizes as soon as the flood reaches its maximum level. In the riparian belt, the groundwater table can fluctuate over a range of 2 m during one season, but in the central part of the island the fluctuations are in order of 0.5 m. Occasionally, a small rise in the groundwater table is recorded during groundwater recession, caused by

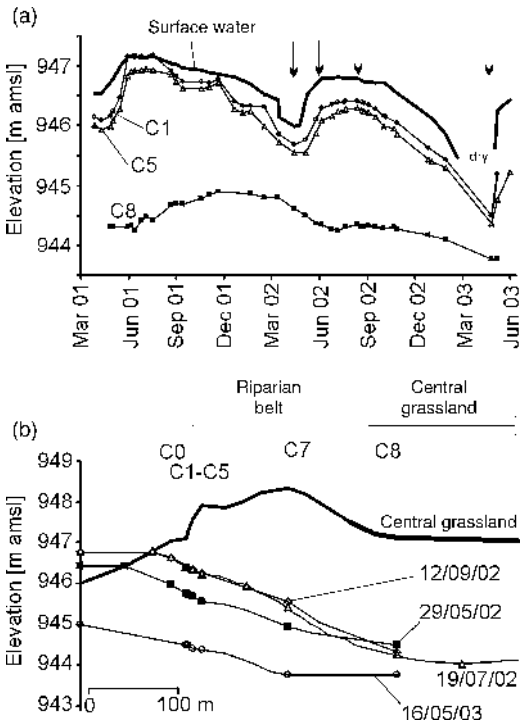

Fig. 3. Groundwater table fluctuations at Camp Island (a) long term hydrographs for selected piezometers (arrows indicate time for which profiles are plotted), (b) groundwater profiles.

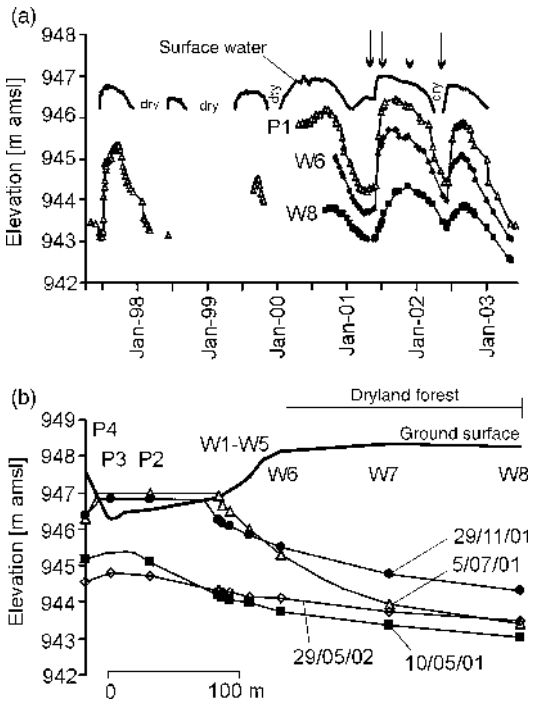

Fig. 4. Groundwater table fluctuations at W1–W8 transect (a) hydrographs for selected piezometers (arrows mark times for which profiles are plotted), (b) groundwater profiles.

direct rainfall recharge, for example in December 2001. As this is the only recharge event observed during the three rainy seasons, rainfall recharge appears to be of limited importance for describing the island's groundwater behaviour. The insignificance of direct rainfall recharge corresponds to low direct rainfall recharge values obtained in the region (e.g. 0–36 mm a^{-1}, Brunner et al., 2004). The important observation is that no groundwater gradient reversal was observed during flood subsidence phase, i.e. groundwater continues to flow from floodplains towards the island throughout the year.

5.2.2. Phelo's and Pan floodplains

The groundwater table in the transect W1–W8 slopes towards the dry land, and this slope is maintained during all seasons (Fig. 4). The response of the island's groundwater table to the arrival of the flood is initially slow and only at a certain stage rapid rise occurs. This is related to the fact that at the arrival of the flood only the central part of the floodplain is inundated, which is approximately 300 m from the island's fringe. During the flood propagation, the front of the surface water moves relatively slowly across the floodplain, as opposed to the relatively fast movement along the longitudinal axis. Hence, the island's groundwater first displays the effects of distant recharge, whereas rapid groundwater rise only occurs when the flood front reaches the direct vicinity of the piezometers. The characteristic feature of this site is that the rise of the groundwater table continues at the far end of the transect throughout the flood season.

The reaction of groundwater to flood is measurable only up to a certain distance from the inundation front. The groundwater level in piezometer F, located in the Pan floodplain at a distance of 500 m from Phelo's floodplain, shows a small rise in 1997, but no reaction in 1998 and a prolonged water table decline in 2002 (Fig. 5). In 2000 and 2001 the Pan floodplain was inundated and rapid rise of groundwater to the surface was

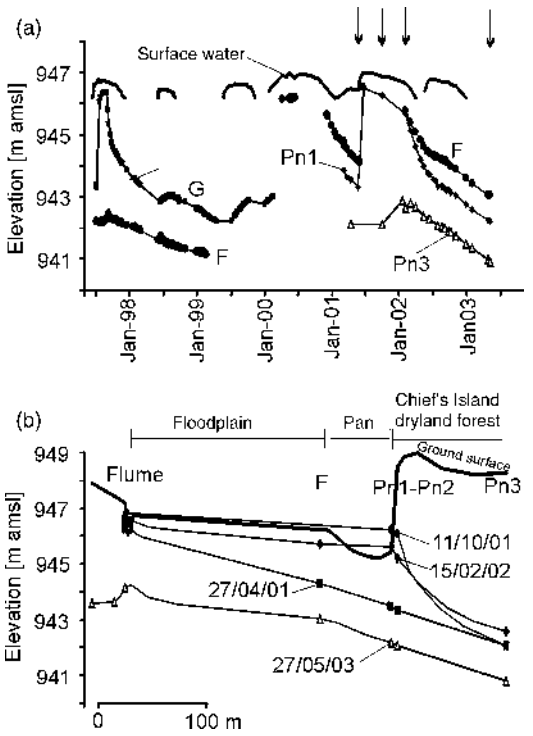

Fig. 5. Groundwater table fluctuations at Pan floodplain, (a) hydrographs for selected piezometers (arrows mark times for which profiles are plotted), (b) groundwater profiles.

observed at that piezometer. The impact of that flooding of the Pan system on the neighbouring dry land can be seen from the groundwater rise at Pn3 piezometer. That rise may reach even further into Chief's Island. Analysis of these groundwater levels indicates, however, that the lateral zone of influence of seasonal flooding on the island groundwater table is limited, and is probably in the order of 500–1000 m.

5.3. Water balance of Phelo's floodplain

Infiltration calculated from the water balance equation is very large amounting to 4300–9700 mm a^{-1}, exceeding 5–9 times the direct evaporation from the flooded area (Table 2). Ramberg et al. (2005) showed that a considerable proportion (60–70%) of that infiltrating water is transferred laterally towards the island bodies by the floodplain-island groundwater flow.

6. Modelling of groundwater flow at Camp Island and Phelo's floodplain

6.1. Camp Island

6.1.1. Model configuration

A transient groundwater model was prepared for the transect C0–C8 located in the SW part of the island, adjacent to the main Boro channel (Fig. 2). Boundaries of the modelled domain were selected at the depression in the island centre, along the flow lines derived from the groundwater table map (obtained from survey of 45 auger holes uniformly distributed over the island) and in the middle of the Boro channel, approximately 300 m from the island's fringe. These were taken as no-flow conditions. The transect was schematised using an array of 40 cells of 10 m by 2 m size. Two layers were used: an upper layer to represent the low permeability island's deposits and a lower one to represent the floodplain aquifer and the sandy aquifer underlying the island. The values of hydraulic conductivity and specific yield/porosity were set to correspond to values obtained from slug tests and laboratory tests (Obakeng and Gieske, 1997; Water Resources Consultants, 2003; see Table 1). For the first layer they were set at 0.5 and 0.05 m d^{-1} for the horizontal and vertical conductivity respectively, and for the second layer values of 5 m d^{-1} and 0.5 m d^{-1} for the horizontal and vertical conductivity respectively.

The simulation period of March 2000 to June 2003 was divided into 36 stress periods. Floodplain bed conductance was calculated assuming a surface layer of 0.5 m thick with a conductivity of 2 m d^{-1}, consistent with the generally observed lack of a clogged layer and results of conductivity measurements by Obakeng and Gieske (1997). To obtain estimates of the extraction depth for the evaporation package, it was considered that it corresponds to groundwater table depth observed at locations devoid of flood for several years. Based on results of our own observations and those by Water Resources Consultants (2003), the extraction depth was set at 3 m in the floodplain and 15 m in the riparian belt. At the island's centre, the extraction depth was set at 3 m, which was expected to reflect the possible depth for which the groundwater table can be effectively tapped through capillary rise and soil evaporation,

considering the predominantly clayey texture of the island's centre soils. Maximum evaporation rates (including transpiration and soil evaporation) were set at 6 mm d^{-1} for the non-inundated floodplain and riparian fringe and 2 mm d^{-1} for the island's centre. The maximum evaporation rate was not varied over time. This was justified by the fact that the maximum potential evaporation rates coincide with the end of the growing season and the rainy season. In such a situation transpiration demand of vegetation is limited by the phenology or satisfied by rain-fed soil moisture. The uptake from groundwater can, therefore, be assumed to be approximately equal throughout the year, and be dependent on groundwater levels only. This assumption is in agreement with the preliminary results of analyses of diurnal groundwater table fluctuations (data not presented here). Rainfall recharge was not simulated in the model as the analysis of groundwater table fluctuations revealed this process to be of minor importance.

6.1.2. Model calibration

The agreement of measured and simulated water levels was achieved by manual adjustment of hydraulic conductivity values. The hydraulic conductivity in the top layer had to be reduced in order to obtain a good simulation of the groundwater table shape. Values of 1–0.01 m d^{-1}, decreasing towards the island centre, were used for horizontal conductivity, with vertical conductivity being an order of magnitude smaller. Also, evaporation in the island's centre had to be increased, because without that it was not possible to obtain groundwater at the island centre at the observed depth. This was done by increasing the extraction depth to 5 m, which effectively increases evaporative uptake and lowers the groundwater table to the level of 4–4.5 m below ground. A similar effect could be achieved by increasing the maximum evaporation rate, but that was considered unrealistic. Fig. 6 presents the comparison of simulated and observed groundwater levels in the modelled transect. The correlation coefficient (r) between the measured (all available measurements) and simulated water levels is 0.71 with a standard error (SE) of 0.32 m.

The model simulates the groundwater table fluctuations well. However, the fluxes in the model are not verified. It is theoretically possible that identical groundwater table fluctuations are obtained

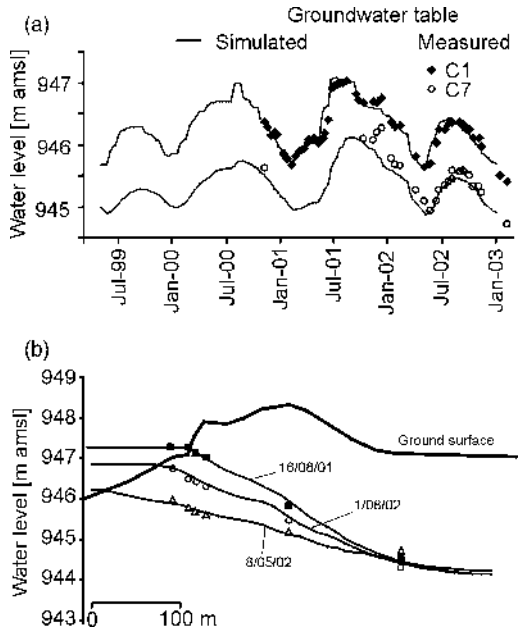

Fig. 6. Comparison of measured and simulated water levels in the Camp transect (a) hydrographs for selected piezometers (b) groundwater profiles.

using a different parameter set and different fluxes. To check the model performance in terms of fluxes, the model-calculated transpiration and soil evaporation values were thus compared to those obtained from remote sensing data using the SEBAL algorithm (Timmermans et al., 2003 and unpublished data). Model-derived actual transpiration varies from 3.5 mm d^{-1} at the island fringe while soil evaporation in the island centre amounts to 0.7–1.1 m d^{-1}. These values agree well with those obtained from SEBAL for October 2001 (i.e. end of dry season, when most of the evaporation and transpiration stems from groundwater).

6.2. Phelo's floodplain and Pan floodplain

6.2.1. Model configuration

Due to the lack of infiltration estimates for the years when the floodplains of the Pan site were flooded (2000 and 2001) and due to the limited knowledge on the boundaries of the Pan system, it was decided to focus the model on Phelo's floodplain only. The boundaries of the modelled domain were set at such a distance from the floodplain boundary, at

which groundwater table fluctuations resulting from Phelo's floodplain inundation are no longer noticeable, i.e. at approximately 0.8–1.0 km from the floodplain towards the island body. This distance was deduced from the analysis of groundwater table fluctuations in piezometers F and Pn3 and other sites (Water Resources Consultants, 2003). It also corresponds to the width of the belt of vegetation flanking the floodplain that is characterized by the presence of both dry-land and riparian species and a slightly higher vegetation density compared to dry-land woodland covering the central part of Chief's Island (visible in Fig. 2), indicating the influence of shallow groundwater. The boundary was simulated in the model using a no-flow boundary condition.

The modelled domain was schematized using a square grid with cells of 20 m by 20 m. The groundwater aquifer is represented by a single layer of 60 m depth (this depth was earlier established in a modelling exercise to accommodate 95% of groundwater discharge across a 300 m deep uniform aquifer with the groundwater table gradients as observed in Phelo's floodplain). Transpiration uptake by vegetation, both within the islands and on the non-flooded floodplains is taken into account, and represented in a similar way as for Camp Island. The simulation period of June 1997-August 2003 is divided into 29 periods, each representing either a no-flood or a different flood level condition. The extent of inundation, simulated by the river package, was varied in time according to the flood extent determined from the topographical map and the water levels at the inlet of the floodplain. The no-flood periods are simulated by removing the river package.

Little justification can be found *a priori* for applying a spatially varying distribution of hydraulic parameters. Hence, a uniformly distributed hydraulic conductivity of 5 m d^{-1} and a specific yield of 0.20 were used as initial values. A maximum potential evaporation rate was set uniformly over the simulation period at 3 mm d^{-1} for dry-lands (that was less than in the case of Camp Island due to lower density of riparian vegetation), but was kept at 6 mm d^{-1} for the non-inundated floodplains. The extraction depth was set at 3 m for floodplains and at 15 m for woodlands. Water levels in the cells representing an inundated floodplain (head-dependent flow boundary) were set for each simulation period at the observed values. Floodplain bed conductance was calculated assuming a surface layer of 0.5 m thick with a conductivity of 2 m d^{-1}, consistent with results by Obakeng and Gieske (1997).

6.2.2. Model calibration

The model was calibrated against the measured groundwater levels and infiltration (the latter is simply the amount of water contributed to the groundwater by head-dependent flow boundary cells). The calibration was done manually by adjusting the transmissivity of the aquifer (by reducing aquifer depth to 15 m) and the maximum evaporation rate (it had to be reduced to the value of 2 mm d^{-1} for dry-lands). Fig. 7 presents a comparison between simulated and measured groundwater levels ($r=0.69$ and SE of 0.29 m). Fig. 8a and b present comparisons between simulated and measured infiltration, on an annual ($r=0.99$ and SE $=0.07$ Mm^3) and monthly basis ($r=0.85$, SE $=3230$ m^3 d^{-1}), respectively. The observed and simulated water levels and infiltration correspond rather well. Only the peak infiltration appears larger in the model compared to the water balance derived value. This discrepancy probably results from the model not accounting for residual moisture in the aeration zone above the groundwater table, remaining after the previous flood event and replenished during the rainy season. As a result the model requires more infiltration for the water table to rise to the surface, compared to what is observed in reality. However, as this has little effect on the main process of interest, i.e. floodplain-island groundwater flows, it was decided not to correct for it at this stage.

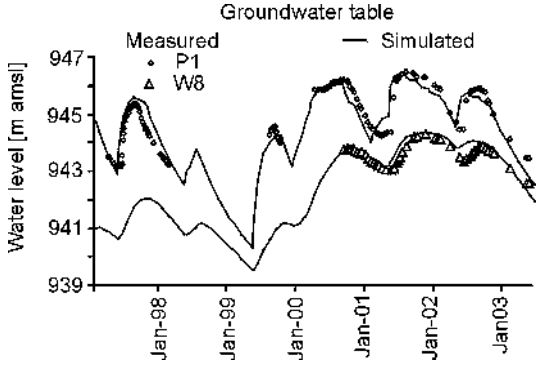

Fig. 7. Comparison of measured and simulated groundwater levels at selected piezometers for Phelo's floodplain model.

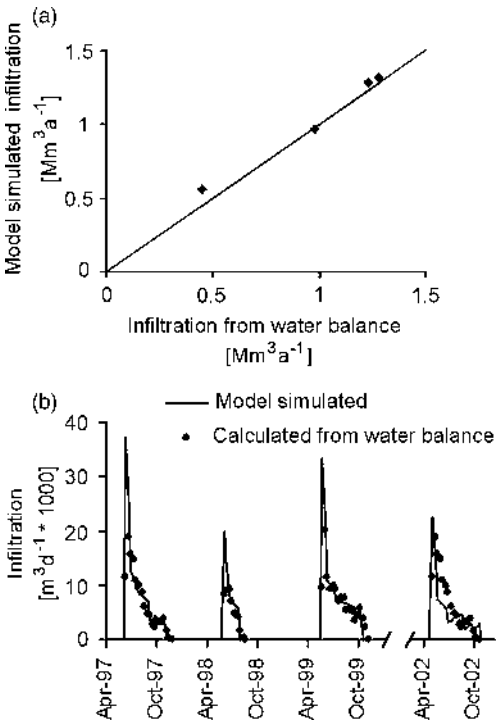

Fig. 8. Comparison of infiltration simulated by Phelo's floodplain model with that calculated from water balance.

Similarly to the Camp Island model, comparison of the computed transpiration and evaporation with SEBAL-derived evaporation was used for the purpose of verification. Average island transpiration and evaporation rates in the order of 1–2 mm d^{-1} were obtained from the model. Overall evaporation rates obtained by SEBAL for October 2001 (Timmermans et al., 2003 and unpublished data) fell within the same range.

7. Results of the groundwater models

7.1. Camp Island

7.1.1. Seasonal dynamics of floodplain-island groundwater flow

Flow between floodplain and island (i.e. across the island boundary) calculated from the model, expressed in m^3 d^{-1} per unit length of shoreline, is presented in Fig. 9. A regular pattern is observed of increase at the arrival of the flood with a subsequent slow decrease throughout the advanced flood and flood subsidence periods. Peak flow rates during the rise of the flood are in the order of 0.55–0.6 m^3 d^{-1} m^{-1}. It appears, however, that flow rates in the dry period before the flood arrival are also substantial, in the order

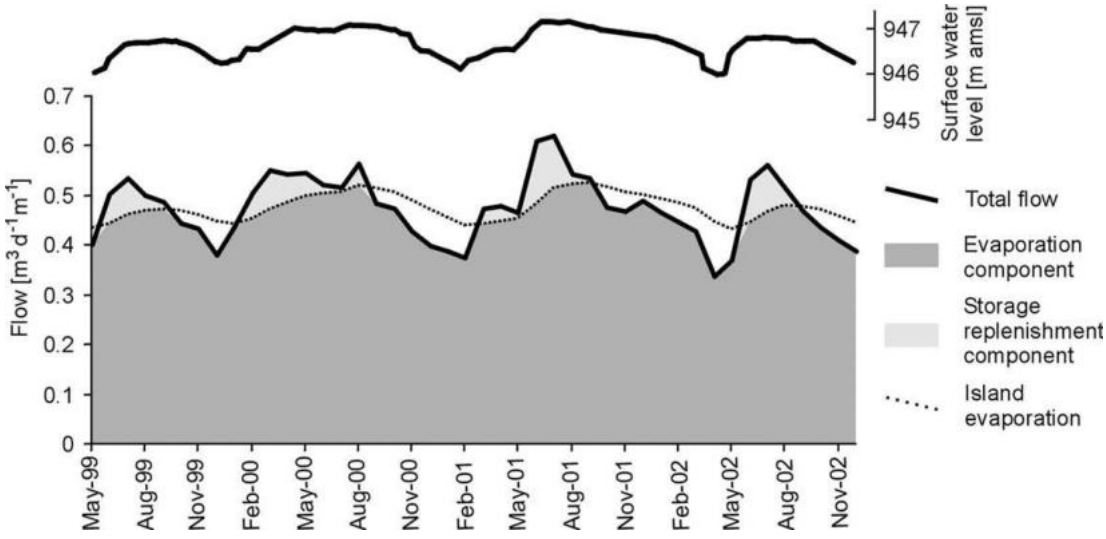

Fig. 9. Components of floodplain-island groundwater flow for the Camp Island model.

of 0.4–0.5 $m^3\,d^{-1}\,m^{-1}$. This remarkable phenomenon can be explained by splitting the flux across the floodplain-island boundary into two components: 'evaporation' and 'storage replenishment' (Fig. 9). The 'evaporation' component expresses the amount of water flowing across the boundary equal to the evaporation and transpiration from the island groundwater taking place during that same period. The 'storage replenishment' component is the amount of water flowing across the boundary that is equal to the increase of the groundwater storage under the island during that same period. As Fig. 9 shows, 'storage replenishment' component is present only during the flood rising stage. During that period, the groundwater gradient forced by the rising surface water is high enough for the groundwater flow to exceed the evaporative withdrawal, causing a groundwater table rise. During the flood subsidence phase the groundwater flow from the floodplains towards islands is driven by evaporation and transpiration from the island, which remains substantial.

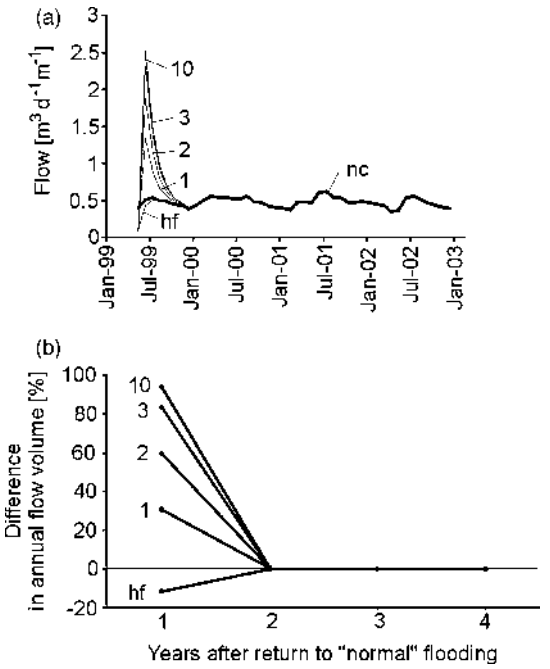

Fig. 10. Camp Island model (a) floodplain-island flow simulated under normal flood conditions (nc), after 1,2,3 and 10 years of no flood and after high flood (hf) conditions. (b) increase in annual floodplain-island groundwater flow volume as compared to the 'normal' flow regime, for the simulated no-flood and high flood antecedent conditions.

7.1.2. Interannual dynamics in floodplain-island groundwater flow at Camp Island

Fig. 10a presents the comparison of the floodplain-island groundwater flow calculated for the 'normal' flood conditions (i.e. time series used in model calibration) and four no-flood and a prolonged flood scenarios. The no-flood period causes a high demand for replenishment and hence increased groundwater flow at the simulated arrival of flood as compared to the 'normal' conditions. The prolonged flood causes a low replenishment demand and hence reduction of flow as compared to the 'normal' conditions. The effect of the antecedent conditions is alleviated within one flooding season, which is clearly seen in Fig. 10b showing the comparison of annual flow volume under 'normal' conditions and under the simulated high flood and no-flood conditions.

7.2. Phelo's floodplain

7.2.1. Seasonal dynamics of floodplain-island groundwater flow at Phelo's floodplain

Flow between floodplain and island (i.e. across the island boundary as shown in Fig. 2) calculated from the model, expressed in $m^3\,d^{-1}$ per unit length of shoreline, is presented in Fig. 11. A similar seasonal pattern to that at the Camp Island is observed: flow increases at the arrival of the flood with a subsequent slow decrease throughout the advanced flood and flood subsidence stage. Flow rates before the flood arrival are in the order of 0.2 $m^3\,d^{-1}\,m^{-1}$, while peak flow rates are in the order of 0.8–2.3 $m^3\,d^{-1}\,m^{-1}$. Similarly to the Camp Island lateral groundwater flow can be split into 'evaporation' and 'storage replenishment' components (Fig. 11).

7.2.2. Interannual dynamics in floodplain-island groundwater flow at Phelo's floodplain

Fig. 12a and b present the results of simulating 1, 2, 3 and 10 years of no-flood and a prolonged high flood condition. Island groundwater storage depleted during a one-year no-flood period is replenished relatively fast: within 1 year. However, the effects of a longer

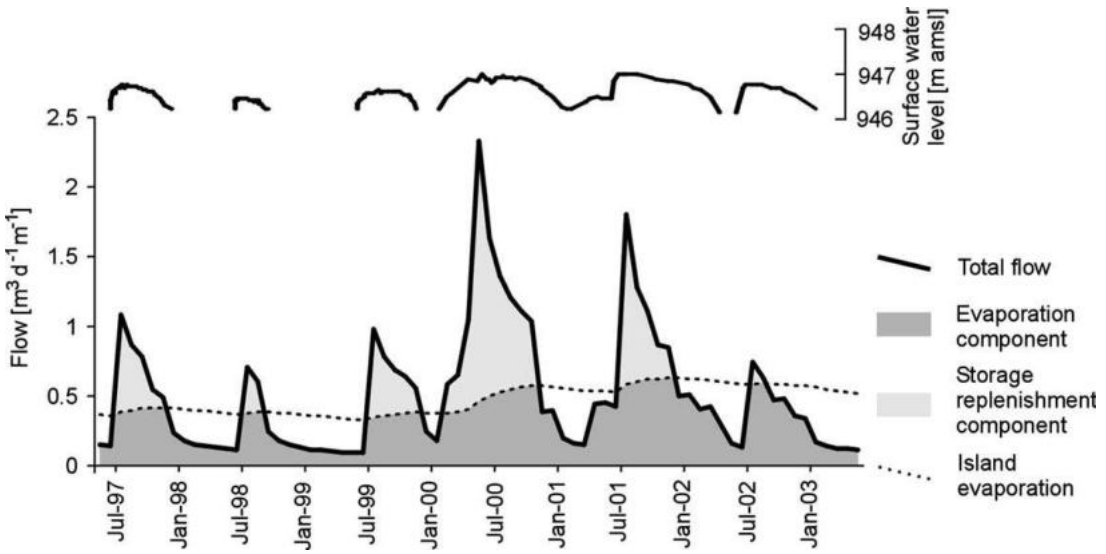

Fig. 11. Components of floodplain-island groundwater flow for Phelo's floodplain model.

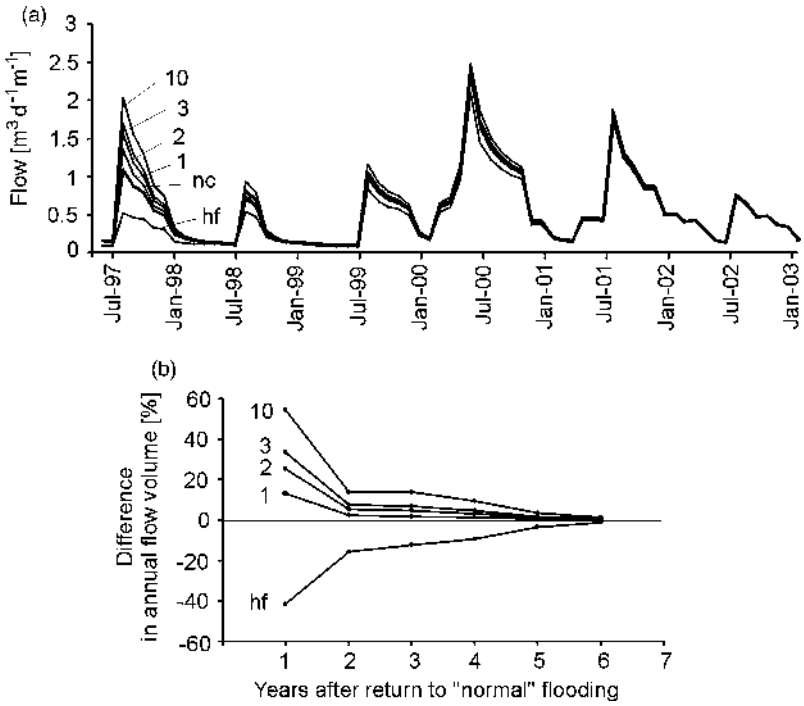

Fig. 12. Phelo's floodplain model (a) floodplain-island flow simulated under normal flood conditions (nc), after 1,2,3 and 10 years of no flood and after high flood (hf) conditions. (b) increase in annual floodplain-island groundwater flow volume as compared to the 'normal' flow regime, for the simulated no-flood and high flood antecedent conditions.

period of no-flood remain visible throughout 4–5 years and longer. The effect of a high and long-lasting flood remains visible during the 5 years after the 'normal' flood regime is introduced.

8. Interpretation and discussion

8.1. Dynamics of floodplain-island groundwater flow

Floodplain-island groundwater flow displays a certain degree of similarity for the two sites analysed, and, based on that, a general understanding of the dynamics of this interaction in the Okavango Delta can be obtained. The seasonal variation of floodplain-island groundwater flow is the effect of the superposition of a relatively constant evaporation and transpiration demand from island groundwater on the flood-induced replenishment of groundwater storage under the island. On the arrival of the flood, the floodplain groundwater table is usually at a certain depth (Fig. 13a). Infiltration occurs at the flood front with inverse saturation, a process analogous to infiltration in disconnected ephemeral rivers (Stephens, 1996). Observations indicate that in the Okavango Delta it takes several hours to 3 days before the percolation front connects to the floodplain groundwater table (Obakeng and Gieske, 1997; Wolski and Savenije, 2003). Considering the time scales at which the variation of groundwater flow between floodplains and islands is observed, i.e. several days to months, this rapid infiltration is not of concern for the main topic of this paper. As a result of the rise of the groundwater table in the floodplain, the groundwater gradient between floodplain and island increases, causing increased groundwater flow towards the island centre (Fig. 13b). At a certain point the flow exceeds evaporation and island groundwater storage starts to be replenished. During the stable flood phase, the rate of lateral groundwater flow starts to decline as the island groundwater storage is filled up (Fig. 13c). At that point, an equilibrium situation occurs where the lateral groundwater flow is equal to the actual transpiration by vegetation and bare soil evaporation from the island. During flood subsidence, the surface water level drops and so does the floodplain-island groundwater level gradient and groundwater flow (Fig. 13d). As a consequence, evaporation draws mainly from island groundwater storage, causing a lowering of the groundwater table. A small gradient towards the island remains, which maintains the flow between floodplain and island.

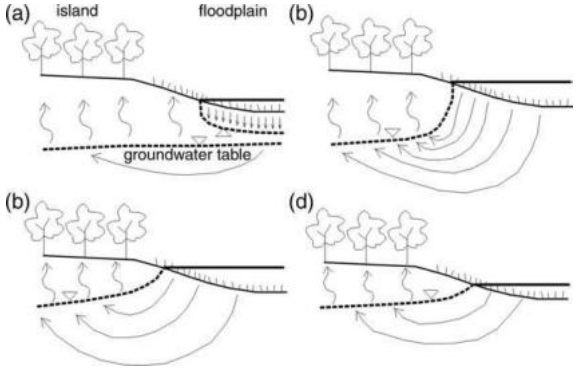

Fig. 13. Schematic representation of a floodplain-island groundwater system. Arrows indicate groundwater and transpiration fluxes.

8.2. Comparison with other floodplain wetlands

The process described above is a variation of the 'classic' process of response of a phreatic aquifer to a seasonally varying head (stream stage) at its lateral boundary, frequently described in the literature (e.g. Rorabaugh, 1964; Workman et al., 1997; Vekerdy and Meijerink, 1998), often in the context of so-called bank storage (e.g. Barlow et al., 2000; Burt et al., 2002; Chen and Chen, 2003; Whiting and Pomeranets, 1997). In the bank storage process, rising water levels of a stream induce recharge of groundwater and rise in the groundwater table in floodplain, or in the case of inundation of the floodplain, also in the surrounding upland. After recession of the flood, return flow from the groundwater storage towards the stream occurs, or in the case of upland storage, towards the floodplain. In the Okavango Delta, the process is, however, different from that classical bank storage effect. At the sites described here groundwater storage is replenished by flood water, but there is no release from the aquifer storage during the subsiding flood phase, and the flow between the floodplain and an island (effectively an upland) continues. Qualitative observations by McCarthy et al. (1991) and Wolski and Savenije (2003), where the groundwater table under islands remains depressed below the floodplain water

levels indicate that this behaviour is ubiquitous throughout the Delta.

Obviously, the effect of continuous flow from floodplains towards islands is caused by the strong transpiration uptake from the island groundwater table. A consequence of that high transpiration and the lack of return flow between islands and floodplains is that the Okavanago Delta forms a recharge wetland. Although the recharge function of wetlands is often mentioned in general wetland classifications (Mitsch and Gosselink, 2000; Tiner, 1999), examples of wetlands where net recharge takes place, i.e. there is no bank or floodplain storage effect, are rare. Prairie potholes in the northern US and Canada are one of the examples (Hayashi et al., 1998; Winter and Rosenberry, 1995; Winter, 1999), but only those that are in topographically higher positions represent net recharge wetlands (Ferone and Devito, 2004). Interestingly enough, in some cases the recharge role of the prairie potholes is maintained by the phreatophytes (Winter and Rosenberry, 1995). In a case described by Hayashi et al. (1998), as much as 75% of the total water loss from the wetland was caused by transpiration-driven lateral groundwater flow, with the remaining 25% lost to evaporation from the open water surface. This is comparable to the water balance for the Delta floodplain presented by Ramberg et al. (2005) and that in our paper. An African example of a floodplain wetland of a recharge character is the Hadejia-Nguru floodplain on the Niger (Goes, 1999; Thompson and Polet, 2000). However, there are examples of floodplains in a climatic setting apparently favouring recharge conditions, that are not recharge floodplains. The Barotse floodplain of the Zambezi, located in western Zambia only approximately 300 km north of the Okavango, is a discharge wetland (Wolski, 1999), mainly due to higher rainfall (900 mm a^{-1}) and considerable upland recharge (>30 mm a^{-1}). The floodplain of the Murray river in Australia, located in a zone where mean annual rainfall is 200–300 mm and upland groundwater recharge is less than 1 mm a^{-1} is in its natural regime a groundwater discharge feature (Holland et al., 2004). Not many studies, unfortunately, address the issue of controls over the recharge/discharge function of wetlands and in particular floodplains, although it is important for understanding the regional groundwater, as well as for wetland ecology.

8.3. Factors affecting spatial variation in floodplain-island fluxes in the Okavango Delta

The differences between the studied sites manifest themselves in terms of magnitude of floodplain-island groundwater flow and amplitude of seasonal variation. This is in spite of island evaporation demand being similar at both sites (in order of 0.4–0.6 m^3 d^{-1} m^{-1}, Figs. 9 and 11). These differences can be explained by considering differences between the sites in terms of geometry and hydro-period. Phelo's floodplain dries during the low flood season and the floodplain's groundwater storage is relatively small compared to transpiration demand of the surrounding dry-land. As a consequence, the floodplain-island groundwater flow reduces considerably below the island's transpiration demand. Transpiration from the island is satisfied from island groundwater storage instead, and hence a large storage capacity is created to be replenished during the next flood. At Camp Island, there is a considerable storage of groundwater in the Boro river floodplain and water is supplied also by the quasi-permanent Boro river. Therefore, the evaporation demand of the island during the no-flood period is satisfied from floodplain-island groundwater flow, with relatively minor change in island groundwater storage. As a consequence, the storage capacity for the following flood is small, and the overall amplitude of the floodplain-island groundwater flow is small as well. These factors, together with differences in island's evaporation demand, cause system-wide spatial variation in the volumes of water involved and seasonal dynamics of the floodplain-island groundwater flow.

8.4. Consequences for island vegetation

Floodplain-island groundwater flow supplies water to dry-land vegetation. Changes in flooding conditions could therefore affect that vegetation by depriving it of water. In a situation similar to Camp Island, a medium-sized island, the floodplain-island flow has a very dynamic character. During each flood event the island groundwater storage is replenished to the level corresponding to the level of that flood. Hence there is

no progressive reduction in groundwater storage during a series of low floods. Therefore, only during a prolonged drought, involving several years without a flood, is damage of island woody vegetation likely.

In the Phelo's floodplain, however, there is a wide belt of island vegetation, and the groundwater storage underlying it, due to limitations imposed by aquifer properties, could not be filled entirely during a single flood event. In such a situation, a reduction in flood levels or flood duration lasting several years would cause a reduction in island groundwater storage and, as a consequence, would deprive dry-land vegetation of water. A prolonged lack of flood may, therefore, have a potentially serious effect on the vegetation.

In all settings, however, the lack of flood can be compensated by the availability of island groundwater, even if it is not replenished by a flood. The crucial issue in assessing the magnitude of that offset is the depth from which trees can effectively extract groundwater. Although that depth was one of the parameters used in the models presented above (extraction depth), it cannot, unfortunately, be determined accurately from the models. This is so because the models are not very sensitive to that parameter, and a change in that parameter can be compensated for by adjustments of other parameters, without detrimental effects on model performance.

8.5. Effects on flood in the system

The process of floodplain-island groundwater flow, due to the amount of water involved, affects the flooding at the scale of the entire Okavango Delta by reducing the availability of surface water for downstream flooding. The amount of floodwater lost to floodplain-island flow varies from year to year depending on the antecedent flood conditions. The influence of antecedent conditions does not exceed 1 year for medium and small islands (<500 m in width), but for larger islands it may reach 4–5 and more years. In the hydrological models of the Okavango Delta (Dinçer et al., 1987; Scudder et al., 1993; Snowy Mountains Engineering Corporation, 1990) prepared in the past, the process of floodplain-island groundwater flow was not included. The models could not simulate the entire series of observed system outflows properly. This was initially explained by non-stationarity of the system or by errors in model input data. However, Gieske (1997) has shown that the observed variation in Okavango Delta outflows could be simulated better when longer-term antecedent conditions were accounted for, although he did not identify the physical process responsible for that effect. In view of the results presented here, the floodplain-island groundwater flow mechanism can account for the long-term 'memory' of the Okavango Delta hydrological system. It is beyond the scope of this paper to analyse that issue in details, but the results presented here provide a basis for such an analysis, which will be done in the future.

9. Summary

Surface water-groundwater interactions play a crucial role in the hydrology and ecology of the Okavango Delta. In order to evaluate seasonal and long-term dynamics of one of the processes influencing surface water-groundwater interactions, namely the floodplain-island groundwater flow, a network of piezometers located in various settings of the floodplain-island system was monitored. Groundwater table fluctuations observed for up to 6 years were analysed and modelled using groundwater flow models. The floodplain-island groundwater flow varies between 0.2–2.5 $m^3 d^{-1}$ per 1 m of the floodplain/island boundary. The flow is in general very dynamic and driven by island vegetation evaporation and soil transpiration. The seasonal dynamics depends on the evaporation and transpiration demand of an island, the size of the island and hydro-period of the flood in the vicinity of the island. In the case of a typical small to medium sized island (less than 500 m wide), the floodplain-island groundwater flow is not influenced by long-term (more than 1 year) antecedent conditions. In case of regular flooding, the dynamic nature of floodplain-island groundwater flow causes a regular replenishment of island groundwater storage. Only a persistence of no-flood years causes depletion of groundwater storage, and possibly degradation of island vegetation. For large islands (>500 m wide), the influence of long-term antecedent conditions can, however, be visible.

A prolonged reduction in the duration or level of the flood can result in depletion in groundwater storage with negative effects on vegetation. The groundwater flow between floodplains and islands has a potential to affect flooding at the scale of the entire system, and to determine its long-term 'memory'. The results of analyses presented here provide the basis for the assessment of these effects.

Acknowledgements

Work presented here was funded by the University of Botswana as a project named 'Surface water-groundwater interactions in the Okavango Delta', partly financed by the EU in the framework of ICA-4-CT-2001-10040 project. P. Wolski would like to express his gratitude to all who helped with fieldwork during the three years of the project. The valuable suggestions by anonymous reviewers have been highly appreciated.

References

Barlow, P.M., DeSimone, L.A., Moench, A.F., 2000. Aquifer response to stream-stage and recharge variations, II. Convolution method and applications. J. Hydrol. 230, 211–229.

Brunke, M., Gonser, T., 1997. The ecological significance of exchange processes between rivers and groundwater. Freshwater Biol. 37 (1), 1–35.

Brunner, P., Bauer, P., Eugster, M., Kinzelbach, W., 2004. Using remote sensing to regionalize local precipitation recharge rates obtained from the chloride method. J. Hydrol. 294 (4), 241–250.

Burt, T.P., Bates, P.D., Steward, M.D., Claxton, A.J., Anderson, M.G., Price, D.A., 2002. Water table fluctuations within the floodplain of the river severn, England. J. Hydrol. 262, 1–20.

Chen, X., Chen, X., 2003. Stream water infiltration, bank storage, and storage zone changes due to stream-stage fluctuations. J. Hydrol. 280, 246–264.

Chiang, W.H., Kinzelbach, W., 2001. 3-D Groundwater Modelling with PMWIN. Springer p. 346.

Dinçer, T., Child, S., Khupe, B., 1987. A simple mathematical model of a complex hydrologic system - Okavango Swamp, Botswana. J. Hydrol. 93, 41–65.

Doss, P.K., 1993. The nature and dynamics of water table in a system of non-tidal, freshwater coastal wetlands. J. Hydrol. 141, 107–126.

Ellery, K., Ellery, W., 1997. Plants of the Okavango Delta, A Field Guide. Tsaro Publishers, Durban, South Africa p. 225.

Ferone, J.M., Devito, K.J., 2004. Shallow groundwater-surface water interactions in pond-peatland complexes along a boreal plains topographic gradient. J. Hydrol. 292, 75–95.

Freeze, R.A., Cherry, J.A., 1979. Groundwater. Prentice-Hall, Engelwood Cliffs, New Jersey p. 560.

Gieske, A., 1997. Modelling outflow from the Jao/Boro river system in the Okavango Delta, Botswana. J. Hydrol. 193, 214–239.

Goes, B.J.M., 1999. Estimate of shallow groundwater recharge in the Hadeji-Nguru Wetlands, semi-arid northeastern Nigeria. Hydrogeol. J. 7, 294–304.

Hayashi, M., van der Kamp, G., Rudolph, D.L., 1998. Water and solute transfer between a prairie wetland and adjacent uplands, 1. Water balance. J. Hydrol. 207, 42–55.

Hogberg, P., Lindholm, M., Ramberg, L., Hessen, D.O., 2002. Aquatic food web dynamics on a floodplain in the Okavango Delta, Botswana. Hydrobiologia 470, 23–30.

Holland, K., Overton, I., Jolly, I., Walker, G., 2004. An analytical model to predict regional groundwater discharge patterns on the floodplains of semi-arid lowland river. Technical Report 6/04, CSIRO Land and Water, Urrbrae, Australia.

Hughes, F.M.R., 1990. The influence of flooding regimes on forest distribution and composition in the Tana river floodplain, Kenya. J. Appl. Ecol. 27, 475–491.

Krah, M., McCarthy, T.S., Annegarn, H., Ramberg, L., 2004. Airborne dust deposition in the Okavango Delta, Botswana, and its impact on landforms. Earth Surf. Process. Landforms. 29 (5), 565–577.

Kruseman, G.P., 1981. Analysis and Evaluation of Pumping Test Data. ILRI, Wageningen, The Netherlands.

LaBaugh, J.W., Winter, T.C., Adomaitis, V.A., S, G.A., 1987. Hydrology and chemistry of selected prairie wetlands in the cottonwood lake area, Stutsman county, North Dakota. US Geo. Surv. Prof. Paper, 1431.

Maidment, D.R., 1992. Handbook of Hydrology. McGraw-Hill, New York.

McCarthy, T.S., McIver, J.R., Verhagen, B.T., 1991. Groundwater evolution, chemical sedimentation and carbonate brine formation on an island in the Okavango Delta swamp, Botswana. Appl. Geochem. 6 (6), 577–595.

McCarthy, J., Gumbricht, T., McCarthy, T.S., Frost, P.E., Wessels, K., Seidel, F., 2004. Flooding patterns in the Okavango wetland in Botswana, between 1972 and 2000. Ambio 7, 453–457.

McCarthy, T.S., Ellery, W.N., 1995. Sedimentation on the distal reaches of the Okavango fan, Botswana, and its bearing on calcrete and silcrete (ganister) formation. Jsr A: Sediment. Petrology. Proc. A65 (1), 77–90.

McCarthy, T.S., 2005. Groundwater in the wetlands of the Okavango Delta, Botswana, and its contribution to the structure and function of the ecosystem. J. Hydrol. (This issue).

McDonald, M.G., Harbaugh, A.W., 1988. A Modular Three Dimensional Finite Difference Groundwater Flow Model. Technique of water resource investigations, vol. 06-A1. USGS, USA p. 575.

Meyboom, P., 1967. Mass transfer studies to determine the groundwater regime of permanent lakes in hummocky moraine of western Canada. J. Hydrol. 5, 117–142.

Mitsch, W.J., Gosselink, J.G., 2000. Wetlands. Wiley, New York p. 920.

Obakeng, O., Gieske, A., 1997. Hydraulic Conductivity and Transmissivity of a Water-Table Aquifer in the Boro River System, Okavango Delta. Unpublished report. Department of Geological Survey, Lobatse, Botswana.

Ramberg, L., Wolski, P., Krah, M., 2005. Infiltration loss from a seasonal floodplain—a major hydrological process in the Okavango Delta, Botswana. J. Hydrol. (sumbitted).

Rorabaugh, M.I., 1964. Estimating changes in bank storage and groundwater contribution to streamflow. Hydrol. Sci. Bull. 63, 432–441.

Sacks, L.A., Herman, J.S., Konikow, L.F., Vela, A.L., 1992. Seasonal dynamics of groundwater-lake interactions at Doñana national park, Spain. J. Hydrol. 136, 123–254.

Scudder, T., Manley, R.E., Coley, R.W., Davis, R.K., Green, J., Howard, G.W., Lawry, S.W., Martz, D., Rogers, P.P., Taylor, A.R.D., Turner, S.D., White, G.F., Wright, E.P., 1993. The IUCN Review of the Southern Okavango Integrated Water Development Project. IUCN, Gland, Switzerland.

Snowy Mountains Engineering Corporation, 1990.Anon., 1990. Southern Okavango Integrated Water Development Project. Department of Water Affairs, Gaborone, Botswana.

Sophocleous, M., 2002. Interactions between groundwater and surface water: the state of science. Hydrogeol. J. 10, 52–67.

Stephens, D.B., 1996. Vadose Zone Hydrology. Lewis Publishers, Boca Raton, USA p. 339.

Suso, J., Llamas, M.R., 1993. Influence of groundwater development on the Doñana national park ecosystems (Spain). J. Hydrol. 141, 239–269.

Thomas, D.S.G., Shaw, P., 1991. The Kalahari Environment. Cambridge University Press, Cambridge p. 298.

Thompson, J.R., Polet, G., 2000. Hydrology and land use in a sahelian floodplain wetland. Wetlands 20 (4), 639–659.

Timmermans, W., Gieske, A., Wolski, P., Arneth, A., Parodi, G., 2003. Determination of water and heat fluxes with MODIS imagery - Maun, Botswana. In: Owe, M., D'Urso, G., Moreno, J.F., Calera, A. (Eds.), Proceedings of SPIE Vol. 5232, Remote Sensing for Agriculture, Ecosystems and Hydrology. 392 pp.

Tiner, R.W., 1999. Wetland Indicators: A Guide to Wetland Identification, Delineation, Classification, and Mapping. Lewis Publishers, Boca Raton, USA p. 392.

Vekerdy, Z., Meijerink, A.M.J., 1998. Statistical and analytical study of the propagation of flood-induced groundwater rise in an alluvial aquifer. J. Hydrol. 205, 112–125.

Water Resources Consultants, 2003.Anon., 2003. Maun Groundwater Development Project, Project Review Unpublished report. Department of Water Affairs, Gaborone, Botswana.

Weng, P., Sanchez-Perez, J.M., Sauvage, S., Vervier, P., Giraud, F., 2003. Assessment of the quantitative and qualitative buffer function of an alluvial wetland: hydrological modelling of a large floodplain (Garonne River, France). Hydrol. Process. 17 (12), 2375–2392.

Whiting, P.J., Pomeranets, M., 1997. A numerical study of bank storage and its contribution to streamflow. J. Hydrol. 202, 121–136.

Winter, T.C., Rosenberry, D.O., 1995. The interaction of groundwater with prairie pothole wetlands in Cottonwood Lake area, east-central North Dakota, 1979–1990. Wetlands 15, 193–211.

Winter, T.C., 1999. Relation of streams, lakes, and wetlands to groundwater flow systems. Hydrol. Process. 7, 28–45.

Woessner, W.W., 2000. Stream and fluvial plain groundwater interactions: Rescaling hydrogeological thought. Ground Water 38 (3), 423–429.

Wolski, P., 1999. Application of reservoir modelling to hydrotopes identified by remote sensing. PhD Thesis, ITC publication 69, ITC, Enschede, The Netherlands, p. 192

Wolski, P., Savenije, H.H.S., 2003. Update of conceptual hydrological model of the Delta. Report to EU funded project ICA-4-CT-2001-10040 no. D2.1, Harry Oppenheimer Okavango Research Centre, Maun, Botswana.

Workman, S.R., Serrano, S.E., Liberty, K., 1997. Development and application of an analytical model of stream/aquifer interaction. J. Hydrol. 200, 149–163.